A&A 549, A37 (2013)
DOI: 10.1051/0004-6361/201220136

Astronomy & Astrophysics

Interstellar H_2 toward HD 147888⋆

P. Gnaciński

Institute of Theoretical Physics and Astrophysics, University of Gdańsk, ul. Wita Stwosza 57, 80-952 Gdańsk, Poland
e-mail: fizpg@univ.gda.pl

Received 31 July 2012 / Accepted 8 November 2012

ABSTRACT

The ultraviolet and far-ultraviolet spectra of HD 147888 allows the H_2 vibrational level $\nu = 0$ to be accessed along with higher vibrational levels of the ground H_2 electronic level. The large number of H_2 absorption lines in the HST spectra allows column densities to be determined even from a noisy spectra. We have determined column densities of the H_2 molecule on vibrational levels $\nu = 0$–5 and rotational levels $J = 0$–6 using the profile fitting method. No variations in the column densities of H_2 on vibrationally excited levels were observed from 2000 through 2009. The ortho to para H_2 ratio $(O/P)^*$ for the excited vibrational states $\nu = 1$–4 equals to 1.13. For the lowest vibrational state $\nu = 0$ and rotational level $J = 1$ the ortho to para H_2 ratio is only 0.15. The temperature of ortho-para thermodynamical equilibrium is $T_{OP} = 42 \pm 3$ K.
The measurements of H_2 column densities on excited vibrational levels (from the HST spectra) leads to constraints on the radiation field in photon-dominated region (PDR) models of the interstellar cloud towards HD 147888. The Meudon PDR model locates the cloud 0.62 pc from the star. The modeled hydrogen cloud density (89–336 cm^{-3}) agrees with independent density estimations based on the C_2 molecule and the chemical model. The observed $(O/P)_{J=1}$ and $(O/P)^*$ H_2 ratios cannot be explained by a simple model.

Key words. ISM: clouds – ISM: molecules – ultraviolet: ISM

1. Introduction

The molecular hydrogen is the most common molecule in the interstellar medium. The H_2 molecule in the ground electronic state does not have a permanent dipole moment, hence no dipole-allowed vibrational or rotational transitions. Consequently, the observations of H_2 emission lines from cold molecular clouds are difficult. The H_2 molecule can, however, be observed in the lowest rotational levels (up to $J = 5$–8) of the ground electronic and vibrational level ($\nu = 0$) by its ultraviolet absorption spectrum. The H_2 molecules are formed on the surface of dust grains. However, the distribution of newly formed H_2 molecules on energy levels is not known exactly. The absorption lines of molecular hydrogen in the Lyman and Werner bands are in the UV and far-UV ranges, observed, for example, by the FUSE (Far Ultraviolet Spectroscopic Explorer) and HST (*Hubble* Space Telescope) satellites. The fluorescence that follows the absorption leads then to populating the ro-vibrational levels of the ground electronic level. The later decay by quadrupole transitions is seen as emission in the infrared spectral range. A detailed description of these processes was presented by Black & Dalgarno (1976). The H_2 IR and UV emission lines have been detected in various astronomical objects, such as planetary nebula, SNR, clusters of galaxies, AGN, starburst regions, T Tauri stars, circumstellar disks, and planetary atmospheres.

Observations of molecular hydrogen in vibrationally excited levels ($\nu \geq 1$) can be used to distinguish shock-heated gas from gas heated by the far-ultraviolet radiation field. First detection of interstellar H_2 absorption lines from vibrationally excited levels (H_2*) was performed by Federman et al. (1995) in an HST spectrum of ζ Oph. A rich spectrum of vibrationally excited hydrogen molecule was described by Meyer et al. (2001) in the HST/STIS (Space Telescope Imaging Spectrograph) spectrum of HD 37903. Based on the nonthermal population of H_2 energy states and the constancy of H_2 line velocities and line widths they concluded that the H_2 excitation arises through UV fluorescence and not through shock heating. Meyer et al. (2001) have also noticed that vibrationally excited H_2 is present in the cloud towards HD 147888. The presence of both FUSE and HST/STIS spectra for HD 147888 (ρ Oph D) gives us a rare opportunity to measure the column density of H_2 energy levels excited by fluorescence ($\nu \gg 0$) and by other processes (collisions, formation, and fluorescence) on the $\nu = 0$ level. As a consequence, we can calculate a photon-dominated region (PDR) model that is well constrained by density and by the ultraviolet radiation flux (star-cloud distance).

In a previous paper (Gnaciński 2011), the H_2 observations from the HST and FUSE satellites toward HD 37903 were analyzed. The sightline toward HD 147888 is the second and last sightline where H_2 lines from $\nu = 0$ (FUSE) and from vibrationally excited (HST) levels were observed. Their weakness meant that the H_2* absorption lines from vibrationally excited levels toward HD 147888 were not analyzed previously. We present the first determination of H_2* column densities toward HD 147888 and a PDR model based on H_2 column densities on the $\nu = 0$ and on vibrationally excited levels. Our PDR model significantly differs from the previously calculated model and agrees with independent determinations of hydrogen density. The two other sightlines toward which Meyer et al. (2001) have

⋆ Based on observations made with the NASA/ESA *Hubble* Space Telescope and with NASA/Johns Hopkins University Far Ultraviolet Spectroscopic Explorer, obtained from the data archive at the Space Telescope Science Institute. STScI is operated by the Association of Universities for Research in Astronomy, Inc. under NASA contract NAS 5-26555. Support for FUSE data is provided by the NASA Office of Space Science via grant NAG5-7584 and by other grants and contracts.

detected H_2* absorption lines, namely HD 37021 and HD 37061, do not have FUSE spectra, therefore determination of H_2 column densities on the basic vibrational $v = 0$ level is impossible for these two sightlines.

The interstellar H_2 plays a fundamental role in gas chemistry. The H_2 molecule is the key reagent in many chemical reactions leading to produce heavier molecules. Many chemical reactions need activation energy or are endothermic. The internal energy of H_2 on rotationally and vibrationally excited levels can lead to overcoming the energy barrier. In this way the presence of H_2 on excited states influences the reactions' rate coefficients and the chemistry in interstellar clouds. For many reactions the H_2* on vibrationally excited levels has significantly higher reactions rate than on the basic $v = 0$ level. The rate coefficients at 100 K for reaction $O + H_2 \rightarrow OH + H$ increases by 11 orders of magnitude for the $v = 3$ vibrational state as compared to the $v = 0$ level (Sultanov & Balakrishnan 2005). Also the formation of CH^+ in the reaction $H_2 + C^+ \rightarrow CH^+ + H$ is ten orders of magnitude higher for H_2* than for the H_2 ground level (at 200 K) (Agúndez et al. 2010). The methylidyne cation (CH^+) formed easily in reactions with H_2* reacts again with H_2, forming CH_2^+ and CH_3^+ in exotermic reactions. In hot PDRs with large FUV exposition, as for HD 34078 or the Orion Bar, forming of CH^+ in reactions with H_2* is the dominant path to producing the methylidyne cation (Agúndez et al. 2010).

Also the ortho-to-para (hereafter O/P) H_2 ratio influences the chemical reaction rate. The reactions involving deuterated species are particularly affected (Pineau des Forêts et al. 1991). The degree of deuteration of molecules in dense interstellar clouds is correlated with the O/P H_2 ratio. The correlation is caused by the proton-exchange reactions, such as $HD + H^+ \rightleftarrows H_2 + D^+$ or $HD + H_3^+ \rightleftarrows H_2 + H_2D^+$, which produce H_2 in $J = 0$ and $J = 1$ states, depending on input energies (Pineau des Forêts et al. 1991).

The H_2 column densities in the direction of HD 147888 for the two lowest rotational levels, $J = 0$ and $J = 1$, have been derived by Rachford et al. (2009) using the FUSE spectra. These spectra of 22 stars were also used by Jensen et al. (2010) to derive column densities of rotational excited molecular hydrogen. Interstellar H_2 toward HD 147888 was detected by them up to rotational level $J = 6$. A Meudon PDR model for the cloud toward HD 147888 was also calculated by Jensen et al. (2010). The H_2 and CO column densities toward HD 147888 were derived by Sheffer et al. (2008) from the FUSE and HST/STIS spectra. The HST/STIS spectra of HD 147888 was also used by Sonnentrucker et al. (2007) to determine the column densities and rotational excitations of CO and C_2. The high-resolution optical spectra of CN, CH, CH^+, Ca I, K I and Ca II absorption lines toward HD 147888 were analyzed by Pan et al. (2004).

Snow et al. (2008) have analyzed the spatial distribution of stars in the ρ Oph cloud complex. Based on the Hipparcos parallaxes and absorption lines of Na I, K I, and Ca II, they estimated the distance to the molecular cloud to be 122 ± 8 pc. The stars ρ Oph A (HD 147933) and ρ Oph D (HD 147888) have similar column densities for K I, CH, and CN. Both stars are located in front of the densest part of the cloud, which is seen as a reflection nebula associated with ρ Oph A. The star ρ Oph C is located behind this cloud.

In Sect. 2 we present the HST and FUSE observations of HD 147888. The details of H_2 column densities calculations are also described in Sect. 2. In Sect. 3 we analyze the noise robustness of the fit to the HST spectrum. Section 4 presents the derivation of ortho/para H_2 ratio and temperatures calculated from the H_2 molecule. The calculated PDR models are presented in Sect. 5 and discussed in Sect. 6.

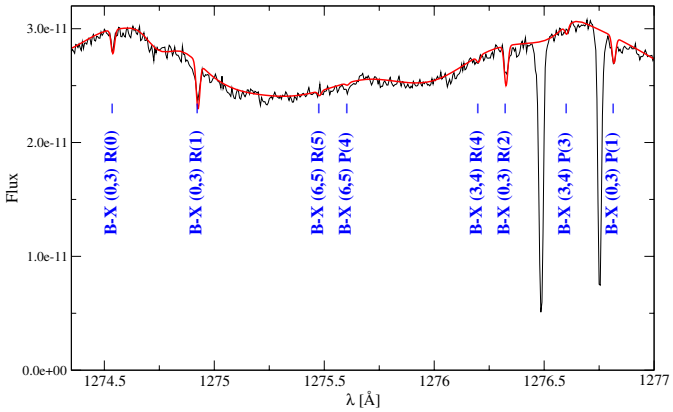

Fig. 1. A fragment of the average HST spectrum. The synthetic spectrum (thick line) was fit to the whole HST spectrum. The Doppler broadening parameter was set to $b = 2.5$ km s^{-1}. The two deep absorption lines are C I lines.

2. Observations and data analysis

We have used HST/STIS spectrum o59s05010 made 17 Aug. 2000 and spectra made on 2 Oct. 2009 (ob2602010 and ob2602020) to obtain column densities on vibrationally excited H_2 levels. No systematic differences were found between the two observations. Therefore all STIS spectra were combined into a single spectrum ranging from 1145 Å to 1356.8 Å. The STIS spectra were coadded using linear interpolation and a fixed step in wavelength of 0.005 Å. The column densities on the ground vibrational level ($v = 0$) were determined from the FUSE spectra P1161501016–19. These spectra were averaged using the IRAF tasks *poffsets* and *specalign*. The FUSE spectrum extends from 904 Å to 1188 Å. We used FUSE spectra from the detectors LiF 2a and LiF 1a that have the best quality.

The column densities were derived using a program developed by the author. It uses the profile fitting method. The *amoeba* procedure described in Press et al. (2007) was used for minimization of the multidimensional function $\sum_i (F_{\rm obs}(\lambda_i) - F_{\rm fit}(\lambda_i; v, b, N_1, N_2, \ldots))^2$, where λ_i are wavelengths in the observed spectrum $F_{\rm obs}$, v is the cloud velocity, b stands for doppler broadening, and N are column densities of various H_2 ro-vibrational levels. The Voigt profile was calculated using the procedure developed by Shippony & Read (1993). The convolution with instrumental PSF was calculated using the routines from Press et al. (2007). The stellar continuum was modeled independently from interstellar line fitting. The continuum was formed by cubic spline functions passing through manually placed continuum points.

The whole HST/STIS spectrum was fit at once with a synthetic spectrum that included 440 H_2 absorption lines. The cloud velocity and column densities of all vibrationally and rotationally excited levels were free parameters. The H_2 spectral line positions and oscillator strengths were adopted from the MOLAT Atomic and Molecular Data[a] database. The PSF function for HST/STIS spectrum was interpolated from tables presented by Kim Quijano et al. (2003) at wavelength 1242 Å (middle of the STIS spectrum). A fragment of HST spectrum together with a fit to the whole HST spectrum is shown in Fig. 1.

[a] http://voparis-molecular.obspm.fr/index.php?page=pages/slap.php

Table 1. Column densities of the H_2 ro-vibrational levels towards HD 147888 [log cm^{-2}].

$J\backslash v$	0	1	2	3	4	5
0	**20.50** ± 0.03	**13.17** ± 0.06 (1)	**12.49** ± 0.03 (4)	**12.03** ± 0.04 (5)	**11.90** ± 0.04 (11)	**12.04** ± 0.06 (12)
1	**19.68** ± 0.10	13.52 ± 0.03 (3)	**12.84** ± 0.04 (6)	**12.58** ± 0.03 (14)	**12.25** ± 0.04 (20)	**12.42** ± 0.05 (27)
2	**18.74** ± 0.06	**13.55** ± 0.02 (4)	**12.80** ± 0.04 (7)	**12.53** ± 0.04 (15)	**12.41** ± 0.03 (22)	12.16 ± 0.03 (32)
3	**17.11** ± 0.25	**13.45** ± 0.02 (4)	**12.73** ± 0.03 (7)	**12.43** ± 0.02 (15)	**12.31** ± 0.02 (27)	12.28 ± 0.05 (29)
4	**15.67** ± 0.30	13.09 ± 0.04 (4)	**12.58** ± 0.03 (6)	**12.35** ± 0.05 (16)	**12.09** ± 0.05 (22)	12.00 ± 0.14 (27)
5	**15.00** ± 0.18	13.11 ± 0.06 (3)	12.39 ± 0.03 (8)	**12.21** ± 0.04 (17)	11.90 ± 0.10 (22)	12.23 ± 0.07 (28)
6	**14.07** ± 0.07	–	–	–	–	–

Notes. The absorption lines connected with the column densities marked in bold were clearly seen in the spectrum. Other lines are at the noise level. The errors of HST column densities reflect only the changes in the doppler broadening parameter. The errors in continuum placement can be significant, especially for the lines at noise level. For absorption lines seen in the HST/STIS spectrum the number of lines used for profile fitting is given in parenthesis.

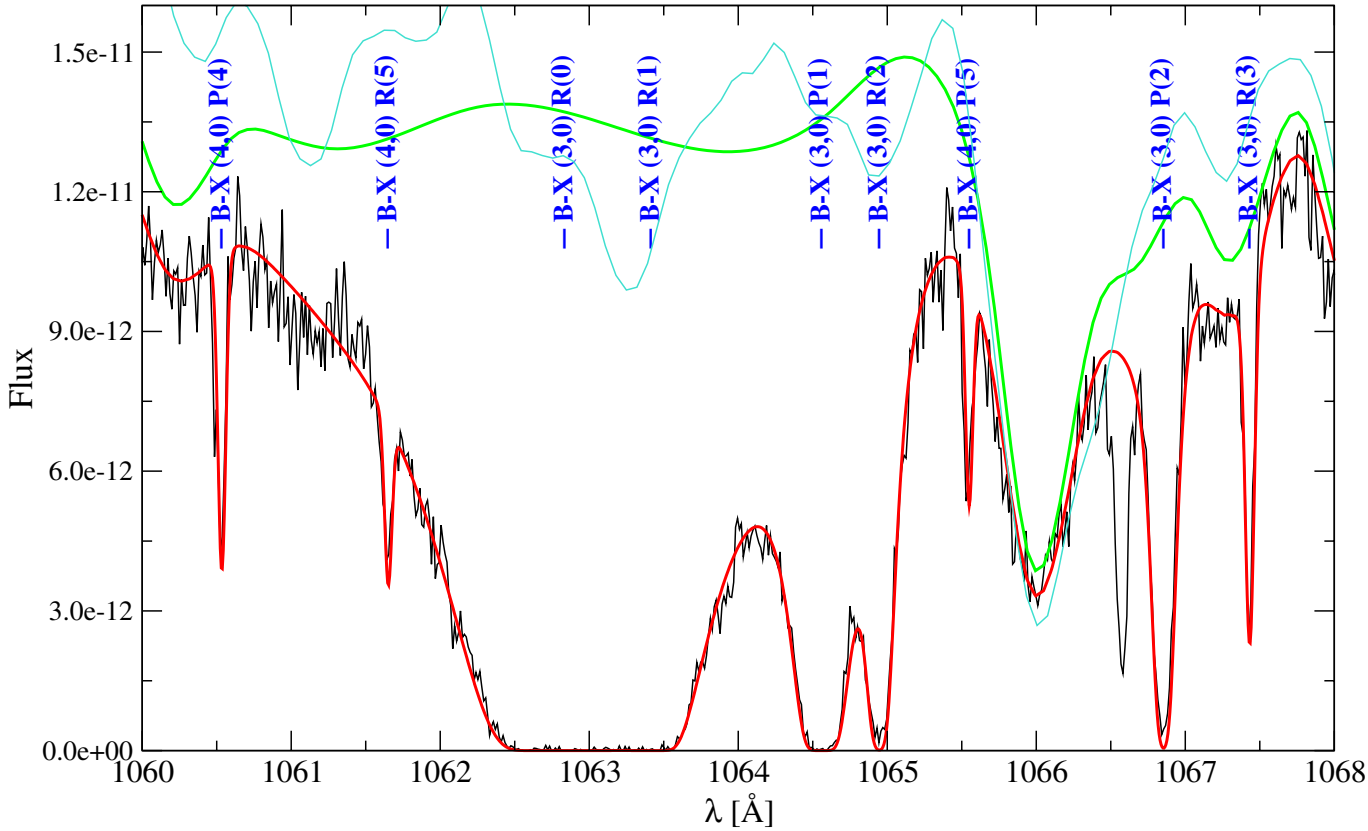

Fig. 2. A fragment of FUSE spectra with the B–X (3,0) transitions of H_2. The upper thick line represents continuum, and the bottom thick line is the simulated spectrum fitted to the observed one. The upper thin line is the stellar synthetic spectrum with rotational and instrumental broadening. The absorption line at 1066.66 Å is an Ar I line.

Fits to STIS spectra were done assuming b = 2.25, 2.5, 2.75, and 3.0 km s^{-1}. Fits done with lower or higher values of b do not match the observed profiles of H_2 absorption lines. Table 1 presents an average column density for four fits with various b values.

Each transition from ground v = 0 J = 0,1 levels to vibrationally excited levels of the B electronic level were fit independently in the FUSE spectrum. We calculated column densities from the following transitions: (0,0), (1,0), (2,0), (3,0), and (4,0). The first digit in parenthesis denotes the upper vibrational level of the B electronic state. The second digit (always 0) is the vibrational level of the ground electronic level X. At each point of the synthetic spectrum optical depths of spectral lines lying closer than 30 Å were summed. The natural line widths were given by Abgrall et al. (2000). The point spread function (PSF) for the FUSE spectra was a Gauss function with $FWHM$ = 15 km s^{-1} (Jensen et al. 2010). A synthetic spectrum, together with the FUSE observation, is shown in Fig. 2.

Fits to the FUSE spectrum were done with Doppler broadenings fixed to b = 2.5 and 3.0 km s^{-1}. As with HST spectra fits with lower or higher values of b do not match the observed profiles of H_2 lines. The continuum level for the FUSE spectra was placed manually in an iterative procedure of fitting column densities and changing the continuum level. There was a slight systematic shift between the observed H_2 line positions and wavelengths from the catalog. Therefore the fitting was performed on small sections of the FUSE spectrum. The derived molecular hydrogen column densities are presented in Table 1

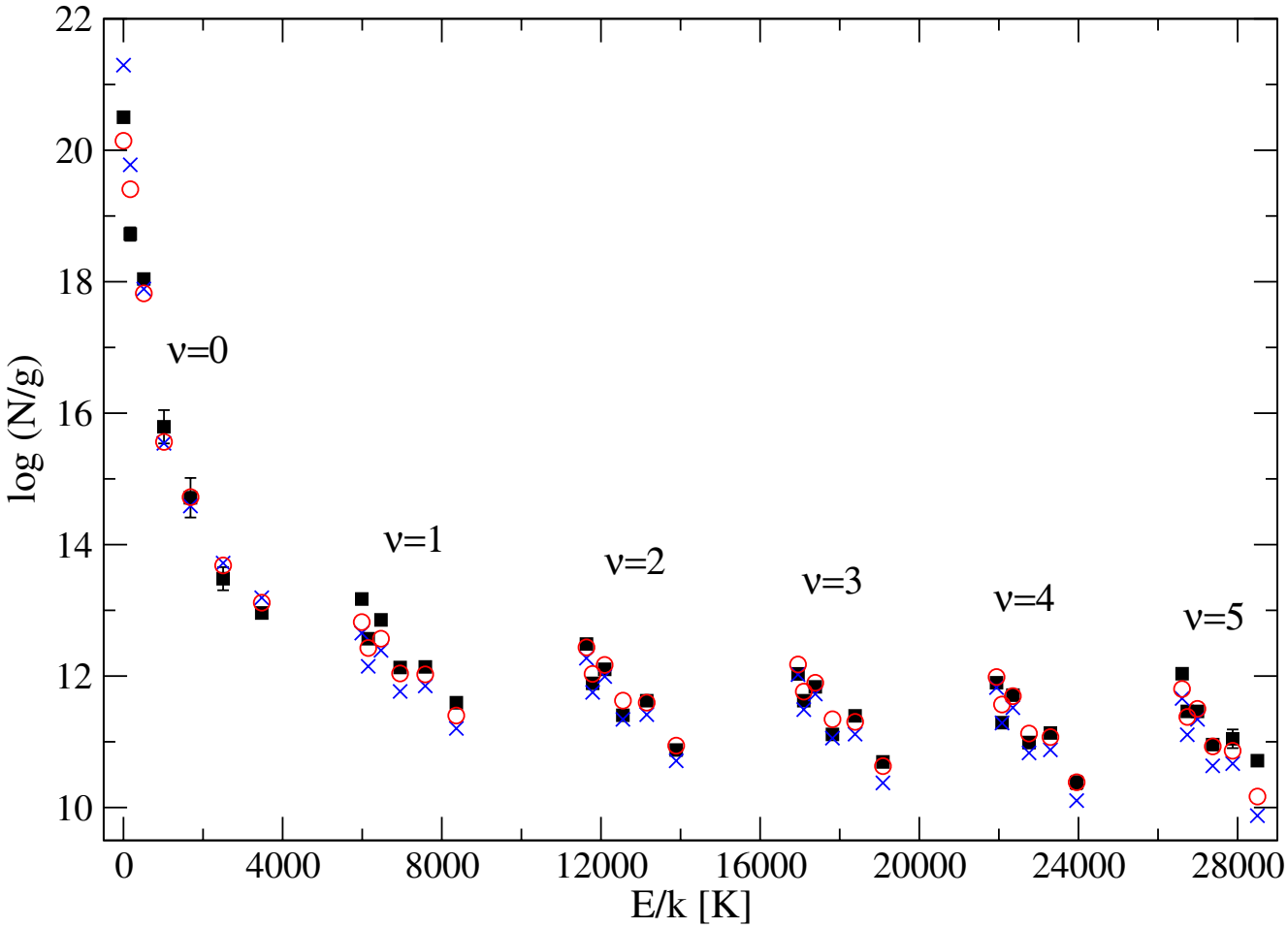

Fig. 3. Logarithms of H_2 column densities divided by statistical weight plotted versus energy (squares with error bar). The v symbol denotes the vibrational quantum number. For $v = 0$ rotational quantum numbers are $J = 0$–6, and $J = 0$–5 for vibrationally excited levels ($v > 0$). The first PDR cloud model is shown as circles. The second model is shown as crosses.

Table 2. Comparison of logarithms of column densities [log cm^{-2}] on the $v = 0$ vibrational level.

	$J = 0$	$J = 1$	$J = 2$	$J = 3$	$J = 4$	$J = 5$	$J = 6$
this paper	20.50 ± 0.03	19.68 ± 0.10	18.74 ± 0.06	17.11 ± 0.25	15.67 ± 0.30	15.00 ± 0.18	14.07 ± 0.37
Jensen et al. (2010)	20.39 ± 0.04	19.71 ± 0.10	$18.51^{+0.02}_{-0.01}$	17.11 ± 0.05	$15.65^{+0.06}_{-0.07}$	$15.13^{+0.09}_{-0.07}$	$14.24^{+0.16}_{-0.18}$

and shown in Fig. 3. Table 1 presents the average logarithms of column densities calculated from various Doppler broadenings and for vibrational transitions (0,0) to (4,0).

To confirm our continuum placement for the FUSE spectrum, we used a synthetic star spectrum from the UVBLUE library (Rodrígez-Merino et al. 2005). The synthetic stellar spectrum from the library was calculated for a star with $T_{\rm eff} = 19\,000$ K, $\log g = 4$, and [M/H] = 0. The synthetic spectrum was convolved with rotational and instrumental (FUSE) broadening functions using the Rotin3[b] program. The stellar rotation velocities catalog (Głębocki & Gnaciński 2005)[c] gives $v \sin i = 175$ km s^{-1} for HD 147888. This rotational velocity is evidently too high. We used the velocity of 100 km s^{-1} to match the observed stellar lines (Fig. 2). Our continuum level, especially the deep absorption line at 1066 Å, is similar to the synthetic stellar spectrum.

Table 2 presents a comparison between derived column densities on the $v = 0$ level and the values derived by Jensen et al. (2010). Our column densities on the $J = 3$ to $J = 6$ rotational levels agree within errors with the Jensen et al. (2010) values that were derived using curve-of-growth methods. The H_2 column density on the $J = 2$ level differs slightly. The spectral lines from the $v = 0$ $J = 2$ levels are saturated, and all methods of column density determinations are inaccurate. The column densities for the $J = 0$ and $J = 1$ rotational levels presented in the Jensen et al. (2010) paper were taken from Rachford et al. (2009). Our H_2 column density on the $v = 0$ $J = 1$ level agrees with the value derived by Rachford et al. (2009). There is, however, a slight difference in column densities for the $J = 0$ level. Rachford et al. (2009) assume a quadratic polynomial continuum, while our continuum uses cubic splines and is similar to the stellar spectrum.

3. Noise robustness

Some of the H_2 absorption lines in the HST spectrum are very shallow or even at the noise level (e.g. absorption lines from

[b] http://nova.astro.umd.edu/Synspec43/synspec-frames-rotin.html

[c] Catalog of Stellar Rotational Velocities, CDS III/244.

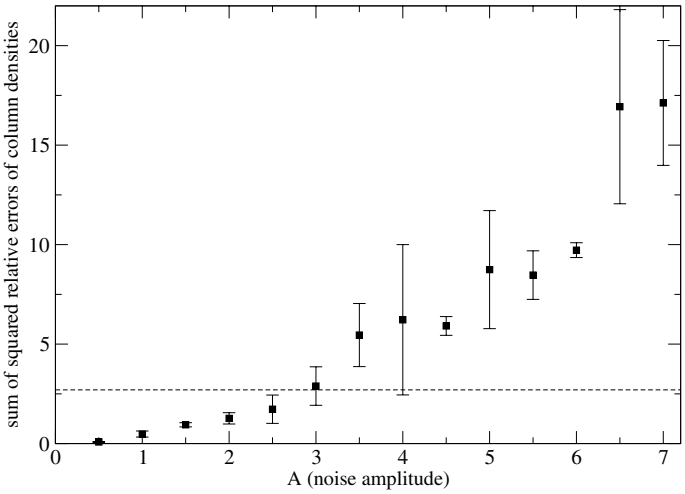

Fig. 4. Robustness of the synthetic spectrum fit to the noisy data. The dashed horizontal line shows errors introduced by changing the original column densities by 30%.

the $v = 1$ level). Therefore we tested the robustness of the fit against noise. The noise observed on the averaged HST/STIS spectrum is about 2.3% at 1256 Å and 0.85% at 1307 Å. We added Gaussian noise of amplitude A to the best fit synthetic spectrum to simulate the noisy spectrum. The points of the generated noisy spectrum are at the same wavelengths as the HST spectrum used previously in the fitting procedure. The Gaussian noise has standard deviation $\sigma = 1$. The spectrum with noise was generated using the formula $F_A = F_{\rm fit}(1 + A * (1.64312 \times 10^{-4} \times \lambda^2 - 0.420740 \times \lambda + 270.283) \times 0.01 \times$ Gaussian Noise), where the factor $(1.64312 \times 10^{-4} \times \lambda^2 - 0.420740 \times \lambda + 270.283)$% reflects the changing noise amplitude in the avaraged HST spectrum. The amplitude $A = 1$ reflects the noise level in the original HST spectrum. The $F_{\rm fit}$ is a synthetic spectrum that represents the best fit to the observed HST/STIS spectra.

Next we performed a fit to the generated spectrum F_A and obtained new column densities by fitting a new synthetic spectrum to the noisy one. All fits to the noisy spectrum were performed with the Doppler broadening parameter fixed to $b = 2.5$ km s^{-1}. The cloud velocity and all column densities for $v \geq 1$ were free parameters. The continuum level was common for all fits. To evaluate the error introduced by noise of various magnitudes A, we calculated a sum of squared relative errors:

$$\sum_{v\geq1,J=0-5} \left(\frac{N_A(v,J) - N_0(v,J)}{N_0(v,J)} \right)^2. \quad (1)$$

The symbol N_A represents column density calculated from the spectrum with noise amplitude A. The generation of a noisy spectrum and subsequent deriving of column densities was repeated three times for each A value. The results are shown in Fig. 4. The uncertainties do not include contribution from continuum placement because the continuum level was kept fixed. They only show the influence of noise on the derived column densities. The energy levels without evident absorption lines gives about 60% contribution to the sum 1. As seen in Fig. 4, even for a noise amplitude two times larger than in the HST spectra, the resulting column densities give the sum of relative errors that is lower than errors introduced by changing the best fit column densities by 30%, so the fitting procedure is robust against the noise.

4. Ortho to para H_2 and temperatures

The column density of atomic and molecular hydrogen toward HD 147888 was initially estimated by Cartledge et al. (2001) based on the hydrogen column densities toward ρ Oph A (HD 147933) determined from *Copernicus* and International Ultraviolet Explorer (IUE) data. We adopted the N(HI) = (5.1 ± 1.1) × 10^{21} cm^{-2} value determined by Cartledge et al. (2004) from the Ly α line in the HST/STIS spectrum of HD 147888. This N(HI) value toward HD 147888 (spectral type B3/B4V) complies with the atomic hydrogen column density toward HD 147933 (B2/B3V). This is not surprising since Snow et al. (2008) shows that HD 147933 and HD 147888 have a similar absorption structure of K I, CH, and CN. Both stars are also at similar distances.

For stars with spectral type B3 or later, the Lyman α line may be contaminated by stellar absorption (Shull & van Steenberg 1985). The adopted hydrogen column density N(HI) is less than the upper limit N(HI) < 5.5 × 10^{21} cm^{-2} derived by Shull & van Steenberg (1985) from IUE spectra. The estimation of hydrogen column density based on interstellar reddening $E(B - V)$ given by Rachford et al. (2009) is, however, almost two times less N(HI) = 2.75 × 10^{21} cm^{-2}.

The total observed column density (see Table 1) of molecular hydrogen is equal to $N(H_2) = (3.7 \pm 0.3) \times 10^{20}$ cm^{-2}. The resulting molecular fraction of hydrogen $f(H_2) = 2N(H_2)/(N(\mathrm{HI}) + 2N(H_2)) = 0.13 \pm 0.03$. The ortho-para H_2 ratio for vibrational levels $v = 1$–4 is $(O/P)^* = 1.13 \pm 0.09$.

The Wilgenbus et al. (2000) method allows calculating the O/P H_2 ratio from an ortho level (J_o) and two adjacent para H_2 levels: $J_o - 1$ and $J_o + 1$. First one should calculate the rotational temperature from the two para H_2 levels:

$$T_{\rm rot} = \frac{E(J_o + 1) - E(J_o - 1)}{k \ln \frac{N(J_o-1)g_J(J_o+1)}{g_J(J_o-1)N(J_o+1)}}. \quad (2)$$

Next we can calculate the O/P ratio:

$$\left(\frac{O}{P}\right)_{J_o} = \frac{Z_o(T_{\rm rot})}{Z_p(T_{\rm rot})} \frac{N(J_o)}{N^{\rm interp}(J_o)}, \quad (3)$$

where $N^{\rm interp}(J_o)$ is the column density of a ortho state interpolated from the two adjacent para states on an $\ln(N(J)/g_J(J))$ against the $E(J)/k$ diagram. The $Z(T)$ are the partition functions for ortho and para H_2. The ortho-para H_2 ratios on the $v = 0$ $J = 1$ and $J = 3$ levels calculated using the Wilgenbus et al. (2000) method are significantly lower than $(O/P)^*$ on vibrationally excited levels. They are equal to $(O/P)_{J=1} = 0.15^{+0.04}_{-0.03}$ and $(O/P)_{J=3} = 0.39^{+0.31}_{-0.17}$. The $J = 5$ ortho level presents O/P as similar to the $(O/P)^*$ on excited vibrationally H_2 levels. The radiative excitation to upper electronic levels is therefore the dominant process for $J < 5$.

Sternberg & Neufeld (1999) have presented a simple model that explains the $(O/P)^*$ H_2 ratio on vibrationally excited levels. They assumed that collisional excitation is negligible to FUV pumping and that collisional de-excitation and photodissociation are negligible to spontaneous radiative decay. Additionally, the H_2 absorption lines from $J = 0,1$ ($v = 0$) should be on the square root part of the curve of growth, as in our case for HD 147888 (see Fig. 2). The damping wings of the H_2 lines lead to the differentiation of ortho and para H_2 on vibrationally excited states ($v > 0$). Under the assumption that local densities of ortho and para H_2 on the ground

level are in LTE ($n_O/n_P = \alpha(T_{gas})$) and the ratio of local densities is equal to the ratio of column densities, the model predicts $(O/P)^* = \sqrt{\alpha(T_{gas})} = \sqrt{(O/P)_{J=1}}$. If on the contrary, the collisions are too rare to maintain the $(O/P)_{J=1}$ in LTE then $(O/P)_{J=1} = \alpha^2(T_{form})$ and $(O/P)^* = \alpha(T_{form})$, where $\alpha(T_{form})$ is the O/P formation ratio on the dust grain surface. This leads again to $(O/P)^* = \sqrt{(O/P)_{J=1}}$ as in previous case. The H_2 in the cloud towards HD 147888 does not satisfy this equation because $1.13 \neq \sqrt{0.15} = 0.39$. Also the cloud toward HD 37903 (see Gnaciński 2011 for O/P H_2 values) does not satisfy the $(O/P)^* = \sqrt{(O/P)_{J=1}}$ equation. One of the reasons for the discrepancy is that the bulk of H_2* and $H_2(J = 0,1)$ are located in different parts of the cloud, so the column densities ratio of H_2* and $H_2(J = 0,1)$ are not equal to the local density ratio. In our PDR cloud model the $n(H_2$*$)$ density is low where $n(H_2)$ is large (observer side of the cloud) and vice versa (Fig. 6).

The temperature of ortho-para H_2 equilibrium T_{OP} was derived from the equation

$$\frac{N(1)}{N(0)} = \frac{g(1)}{g(0)} \exp\left(-\frac{E(1) - E(0)}{kT_{OP}}\right), \quad (4)$$

where $N(J)$ are the column densities, $E(J)$ is the energy on the J level ($v = 0$), and $g(J)$ is the statistical weight

$$g(J) = \begin{cases} (2J+1) & \text{for para } H_2 \text{ (even } J\text{)} \\ 3(2J+1) & \text{for ortho } H_2 \text{ (odd } J\text{).} \end{cases} \quad (5)$$

The temperature of ortho-para H_2 equilibrium $T_{OP} = 42 \pm 3$ K is similar to the value $T_{OP} = 45 \pm 3$ K derived by Jensen et al. (2010). The T_{02} rotational temperature only involves para-H_2 levels and was calculated from an equation that is analogous to Eq. (4). The T_{02} rotational temperature equals 90 ± 3 K (Jensen et al. 2010 gives $T_{02} = 88 \pm 1$ K).

The rotational temperature was also calculated for each vibrational level. The rotational temperature is the inverse of the line slope taken with the minus sign on a plot: $\ln(N/g)$ versus E/k (like Fig. 3 but using a natural logarithm instead of base 10 logarithm). The slope was calculated with the linear regression method separately for ortho and para H_2 spin isomers. The resulting temperatures are presented in Fig. 5. For each vibrational level, the points on the $\ln(N/g)$ versus E/k plot are perfectly placed on a straight line (separately for ortho and para states). The correlation coefficient varies between 0.88 and 1.00. The excellent agreement with the Boltzmann distribution confirms the correctness of the H_2 column densities. For the sightline towards HD 37903, the rotational temperatures fall with increased vibrational number v (Gnaciński 2011). This behavior is not observed towards HD 147888.

5. Models

We used the Meudon PDR code (Le Petit et al. 2006) to calculate the model of the interstellar cloud in front of HD 147888. We calculated isobaric models with exact radiative transfer in all H_2 spectral lines. We calculated 1529 PDR models. The initial hydrogen density in the models was varied from $n_H = 110$ cm^{-3} to 3500 cm^{-3}. The star cloud distance was changed from $d = 0.51$–1.4 pc. The interstellar radiation field on the star side was varied from 1 to 1200 Draine units and was fixed to 1 Draine unit on the observer side. The turbulent velocity was set to $v_{turb} = 2$ km s^{-1} and the star spectral type to B3V. The interstellar reddening $E(B-V) = 0.47$, $R_V = 4.06$, and $A_V = 1.91$ were adopted from Rachford et al. (2009).

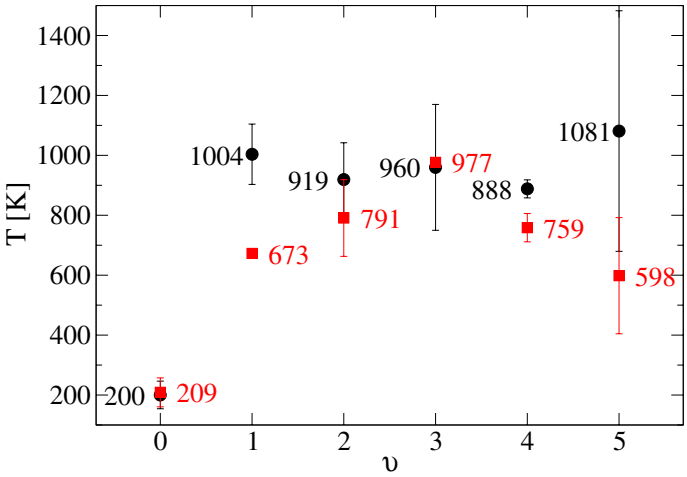

Fig. 5. The rotational temperatures on vibrational levels 0–5. Squares presents rotational temperature of para H_2, while the circles are for ortho–H_2.

The first PDR model was chosen by minimizing the difference in relative H_2 abundances observed in the cloud towards HD 147888 and calculated in a PDR model:

$$\sum_{v,J} w_v \left(\log \frac{N_{obs}(v,J)}{N_{obs}(H_2)} - \log \frac{N_{model}(v,J)}{N_{model}(H_2)}\right)^2. \quad (6)$$

The weights w_v were chosen such that the levels usually excited by fluorescence ($v > 0$) have the same influence on the final sum as the $v = 0$ level excited by collisions and by H_2 formation. The weights w_v were equal to five for $v = 0$ and one otherwise.

The first PDR model has a star-cloud distance of 0.62 pc. The interstellar radiation field on the star side is equal to 700 Draine units. The hydrogen density varies from 89 cm^{-3} on the star side to 336 cm^{-3} near the observer's side. The gas kinetic temperature changes from 358 K on the star side to 98 K on the observer's cloud side. The distance is better constrained than the density. Assuming 1% change of the sum (6) the star-cloud distance can vary up to 10%, while the average density can vary up to 31%. The interstellar radiation field can change by 100 Draine units. In the first cloud model, the ortho/para H_2 ratio for vibrationally excited states equals 1.56. Figure 6 shows that the $(O/P)^*$ ratio on vibrationally excited H_2 levels changes significantly in the cloud. The relative abundance of H_2 on the $v = 1$ level is also shown.

The $(O/P)^*$ curve has a maximum at $A_V = 0.229$ (Fig. 6). Looking from the star side (height A_V), the $(O/P)^*$ rises because the $H_2(J = 1)/H_2(J = 0)$ on the $v = 0$ level gets higher. The ortho H_2 lines are stronger than the para H_2 absorption lines, and at the maximum of (O/P)* at $A_V = 0.229$ selfshielding in the ortho H_2 lines becomes important. Less ortho H_2 is then transferred to the upper electronic levels and the (O/P)* decreases. At the minimum of the (O/P)* curve ($A_V = 0.128$) lines from $J = 0$ and $J = 1$ are both saturated. At the plateau around $A_V = 0.05$, the Lorentzian wings dominate the absorption spectrum.

Our second model was selected by minimizing the difference between the observed and calculated column densities:

$$\sum_{v,J} w_v \left(\log N_{obs}(v,J) - \log N_{model}(v,J)\right)^2. \quad (7)$$

A model chosen using the above formula has to reproduce the H_2 column densities. Our attempts to find a model that satisfies the formula led to an unphysical model for the cloud in front

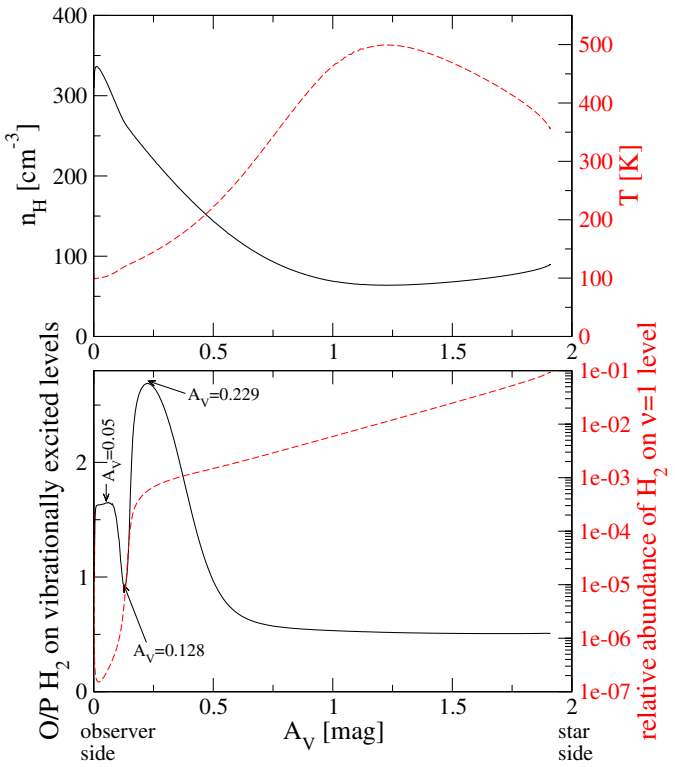

Fig. 6. First cloud model (at $d = 0.62$ pc). The dashed line scale is on the right y-axis. The marked A_V's are discussed in the context of the $(O/P)^*$ variability.

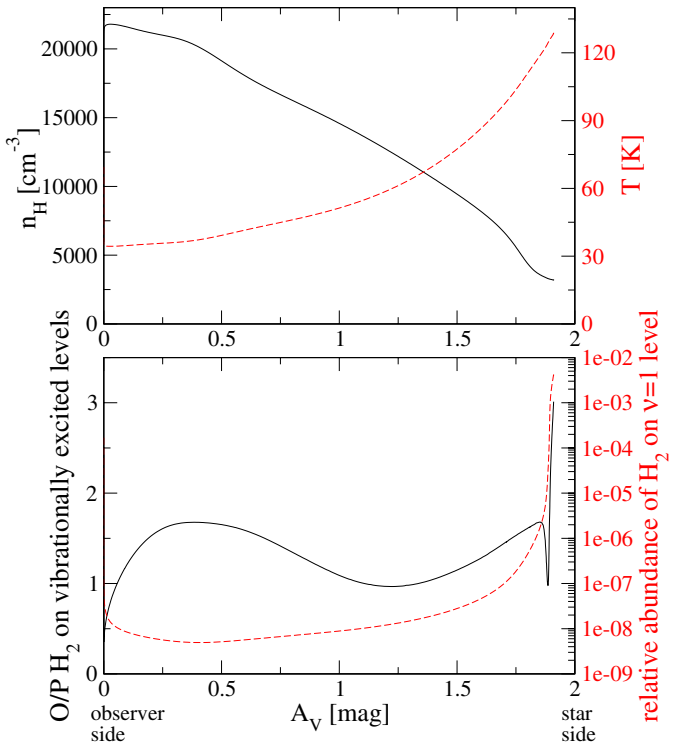

Fig. 7. Second cloud model (at $d = 0.96$ pc). The dashed line scale is on the right y-axis.

of HD 37903. The hydrogen density was higher than 10^6 cm^{-3}. However, we decided to present this model of the cloud towards HD 147888 for comparison purposes, as it has the hydrogen density on the observer's side close to the density presented by Jensen et al. (2010). The PDR model presented by Jensen et al. (2010) has $n_H = 2000$ cm^{-3}. However, their model did not take the H_2 molecules in excited vibrational levels ($v > 0$) into account.

In the second model the hydrogen density varies from $n_H = 22\,000$ cm^{-3} near the observer's side to $n_H = 3200$ cm^{-3} on the star side. The temperature changes from $T = 34$ K to $T = 129$ K, and the interstellar radiation field on the star side is 1 Draine unit. The star-cloud distance in the second model is 0.96 pc. As in the case of the first model, the second model is also better constrained in the star-cloud distance than in density. The 1% change of sum (7) changes the distance up to 5%, while the average density changes by 24%. The interstellar radiation filed on the star side changes at most by 100 Drain units. The ortho/para H_2 ratio in the cloud model equals $(O/P)^* = 1.36$ and the total H_2 column density equals to 2.5×10^{21} cm^{-2}, so the total H_2 column density in this model is about one order of magnitude greater than the observed one. The model H_2 excess is in the $J = 0$ and 1 rotational levels ($v = 0$). These levels are high in order to maintain an adequate population of vibrationally excited states. Figure 7 shows the changes in hydrogen density, gas kinetic temperature, the $(O/P)^*$ H_2 ratio, and the relative abundance of H_2 at the $v = 1$ level.

For both models, the (O/P)* H_2 ratio on excited levels show large spatial variations in the cloud. Column densities of H_2 energy levels in both models are shown in Fig. 3. The input parameters and results of both models are compared with observations in Table 3. Owing to the normalization used in model 1, the total $N(H_2)$ column density is by definition equal to the observed one. However column densities of other species cannot be derived for model 1.

6. Discussion

The CO and C_2 molecules toward HD 147888 were analyzed by Sonnentrucker et al. (2007). The density of hydrogen $n_H = 215^{+55}_{-30}$ cm^{-3} derived from the C_2 rotational levels was calculated by Sonnentrucker et al. (2007) under the assumption of the average Galactic radiation field. Since the radiation field in the cloud toward HD 147888 may be higher, the hydrogen density may also be higher ($n\sigma_0/I \sim$ population of excited rotational levels; van Dishoeck & Black 1982). Nevertheless the derived hydrogen density is similar to hydrogen density in our first model. The C_2 rotational temperature $T_{02} = 38 \pm 20$ K is similar to $T_{OP} = 42 \pm 3$ K as derived from the H_2 molecule.

The density of the interstellar cloud towards HD 147888 was estimated by Pan et al. (2005) on the basis of a chemical model involving CN, CH, C_2, O, C II, and N. Their density $n_H = 425$ cm^{-3} is close to the density derived in our first model. Two independent density estimations thus give densities close to our density in the first PDR model. Therefore we prefer the first model, where the relative H_2 abundances were compared. Pan et al. (2005) have also modeled the CN and C_2 column densities in the direction of ρ Oph D. Both the observed and modeled $N(CN) = 2.1 \times 10^{12}$ cm^{-2}. Our second model gives the CN column density as one order of magnitude higher $N(CN) = 3 \times 10^{13}$ cm^{-2}. The C_2 column density in our second model $N(C_2) = 2.4 \times 10^{15}$ cm^{-2} does not agree with the model by Pan et al. (2005), which give $N(C_2) = 1.9 \times 10^{13}$ cm^{-2}. We cannot derive the denormalized CN and C_2 column densities for our first model due to the normalization used to compute the model.

Table 3. Comparison of observations and models for HD 147888 and HD 37903.

	HD 147888			HD 37903[f]
	Observed	Model 1	Model 2	Model
star-cloud distance	–	0.62 pc	0.96 pc	0.45 pc
interstellar radiation field:				
on the observer's side	–	1 Draine unit	1 Draine unit	1 Draine unit
on the star's side	–	700 Draine units	1 Draine unit	1 Draine unit
hydrogen density	215[a] cm^{-3}, 425[b] cm^{-3}	89–336 cm^{-3}	3200–22 000 cm^{-3}	544–1874 cm^{-3}
gas kinetic temperature	38[c] K, 42[d] K	358–98 K	129–34 K	377–100 K
total $N(H_2)$	3.7×10^{20} cm^{-2}	3.7×10^{20} cm^{-2} [e]	2.5×10^{21} cm^{-2}	9.6×10^{20} cm^{-2} [g]
$f(H_2)$	0.13	–	0.91	0.56[g]
$(O/P)^*$	1.13	1.56	1.36	1.35[g] , 1.57

Notes. [(a)] From C_2 excitation (Sonnentrucker et al. 2007); density may be higher due to higher radiation field. [(b)] From chemical model (Pan et al. 2005). [(c)] T_{02} of C_2 (Sonnentrucker et al. 2007). [(d)] T_{OP} of H_2. [(e)] Equal to observed $N(H_2)$ because of denormalization. [(f)] Gnaciński (2011). [(g)] Observed toward HD 37903.

7. Conclusions

The interstellar cloud towards HD 147888 is one of the rare sightlines where H_2* absorption from vibrationally excited levels is observed. The main results are:

- We have determined H_2 column densities on $v = 0$–5 and $J = 0$–6 from FUSE and HST spectra.
- It is possible to obtain column densities from large numbers of shallow absorption lines arising from the same ground level. The whole HST/STIS spectrum should be fitted at once with a synthetic spectrum to derive column densities from a noisy spectrum.
- The occupation of the vibrationally excited H_2 levels toward HD 147888 did not show any temporal variations over the period of 9 years.
- The ortho-para H_2 ratio on excited vibrational levels $(O/P)^* = 1.13$, while the O/P H_2 on the ground vibrational level $(O/P)_{v=0,J=1} = 0.15$. These ratios do not agree with the simple model by Sternberg & Neufeld (1999).
- The Meudon PDR model (our first model) locates the interstellar cloud 0.62 pc from the HD 147888 star. The hydrogen density in the cloud is 89–336 cm^{-3} and the gas kinetic temperature changes from 98 to 358 K.

Independent density estimations from C_2 and chemical model agree with our model, where the model relative H_2 abundances were compared with relative H_2 abundances from observations (first PDR model).

Acknowledgements. This research was supported by the University of Gdańsk grant BW/5400-5-0336-0 and Polish National Center for Science grant nr 5820/B/H03/2011/40. I would like to thank Herve Abgrall for providing the natural line widths for the H_2 lines.

References

Abgrall, H., Roueff, E., & Drira, I. 2000, A&AS, 141, 297
Agúndez, M., Goicoechea, J. R., Cernicharo, J., Faure, A., & Roueff, E. 2010, ApJ, 713, 662
Black, J. H., & Dalgarno, A. 1976, ApJ, 203, 132
Cartledge, S. I. B., Meyer, D. M., & Lauroesch, J. T. 2001, ApJ, 562, 394
Cartledge, S. I. B., Lauroesch, J. T., Meyer, D. M., & Sofia, U. J. 2004, ApJ, 613, 1037
van Dishoeck, E. F., & Black, J. H. 1982, ApJ, 258, 533
Federman, S. R., Cardelli, J. A., van Dishoeck, E. F., Lambert, D. L., & Black, J. H. 1995, ApJ, 445, 325
Gnaciński, P. 2011, A&A, 532, A122
Jensen, A., Snow, T., Sonneborn, G., & Rachford, B. 2010, ApJ, 711, 1236
Kim Quijano, J., et al., COS/STIS Team 2003, STIS Instrument Handbook (Baltimore: STScI)
Le Petit, F., Nehmé, C., Le Bourlot, J., & Roueff, E. 2006, ApJS, 164, 506
Meyer, D. M., Lauroesch, J. T., Sofia, U. J., Draine, B. T., & Bertoldi, F. 2001, ApJ, 553, L59
Pan, K., Federman, S. R., Cunha, K., Smith, V. V., & Welty, D. E. 2004, ApJS, 151, 313
Pan, K., Federman, S. R., Sheffer, Y., & Andersson, B.-G. 2005, ApJ, 633, 986
Pineau des Forêts, G., Flower, D. R., &McCarroll, R. 1991, MNRAS, 248, 173
Press, W. H., Teukolsky, S. A., Vetterling, W. T., & Flannery, B. P. 2007, Numerical Recipes (Cambridge University Press)
Rachford, B. L., Snow, T. P., Destree, J. D., Ross, T. L., & Ferlet, R. 2009, ApJS, 180, 125
Rodrígez-Merino, L. H., Chavez, M., & Bertone, E. 2005, ApJ, 626, 411
Sheffer, Y., Rogers, M., Federman, S. R., et al. 2008, ApJ, 687, 1075
Shippony, Z., & Read, W. G. 1993, J. Quant. Spectrosc. Radiat. Transf., 50, 635
Shull, J. M., & van Steenberg, M. E. 1985, ApJ, 294, 599
Snow, T. P., & McCall, B. J. 2006, ARA&A, 44, 367
Snow, T. P., Destree, J. D., & Welty, D. E. 2008, ApJ, 679, 512
Sonnentrucker, P., Welty, D. E., Thorburn, J. A., & York, D. G. 2007, ApJS, 168, 58
Sternberg, A., & Neufeld, D. A. 1999, ApJ, 516, 371
Sultanov, R. A., & Balakrishnan, N. 2005, ApJ, 629, 305
Wilgenbus, D., Cabrit, S., Pineau, des Forêts G., & Flower, D. R. 2000, A&A, 356, 1010